

Electronic Supplementary Information

Origin of thermally activated delayed fluorescence in a donor-acceptor type emitter with an optimized nearly planar geometry

Jia-Xiong Chen,^{a,b,c} Ya-Fang Xiao,^b Kai Wang,^{*,a} Xiao-Chun Fan,^a Chen Cao,^b Wen-Cheng Chen,^b Xiang Zhang,^a Yi-Zhong Shi,^a Jia Yu,^a Feng-Xia Geng,^c Xiao-Hong Zhang,^{*,a} and Chun-Sing Lee^{*,b}

^aInstitute of Functional Nano & Soft Materials (FUNSOM) and Jiangsu Key Laboratory for Carbon-Based Functional Materials & Devices, Soochow University, Suzhou, Jiangsu 215123, P.R. China

^bCenter of Super-Diamond and Advanced Films (COSDAF) and Department of Chemistry, City University of Hong Kong, Hong Kong SAR, P.R. China

^cCollege of Energy, Soochow Institute for Energy and Materials Innovations (SIEMIS), Soochow University, Suzhou 215123, P.R. China

Corresponding Author

wkai@suda.edu.cn; xiaohong_zhang@suda.edu.cn; apcslee@cityu.edu.hk.

General information

All compounds were obtained from commercial sources and used as received. ^1H nuclear magnetic resonance (^1H NMR) and ^{13}C NMR spectra were recorded in CD_2Cl_2 and CDCl_3 on Bruker 400 MHz and Bruker 600 MHz spectrometers. Mass spectra data were carried out using Trace-ISQ mass spectrometer. Absorption and photoluminescence (PL) spectra were respectively recorded on a Hitachi UV-Vis spectrophotometer U-3900 and a Hitachi fluorescence spectrometer F-4600. PL transient were recorded by an Edinburgh Instruments FLS980 spectrometer.

Theoretical calculations

All the calculations were performed using Gaussian 09 program package. The ground state geometries were optimized via density functional theory (DFT) at the B3LYP/6-31G* level. Time-dependent DFT (TD-DFT) with B3LYP method for energies and transition properties were then performed in lowest-lying singlet (S_1) and triplet states (T_1) according to the geometry optimization.

Single crystal x-ray crystallography

CCDC 1942309 and 1942310 contain the supplementary crystallographic data for this paper. Single crystal of PXZ-PPO and PXZ-BOO were obtained by solvothermal treatment in chloroform and Hexene, and the data can be obtained free of charge from The Cambridge Crystallographic Data Centre via www.ccdc.cam.ac.uk/data_request/cif.

Device fabrication

Indium Tin Oxide (ITO) glass substrate with a surface resistance of 15Ω was firstly washed with ethanol, acetone and deionized water, and dried in an oven at $100 \text{ }^\circ\text{C}$, then subjected to ultraviolet-ozone system treatment for 10 minutes, finally transferred to vacuum evaporation. At a base pressure of approximately $4 \times 10^{-4} \text{ Pa}$, Hole transport layers, electron transport layers, exciton blocking layers and emitting layers were evaporated onto the ITO substrate at a rate of $1\text{-}2 \text{ \AA/s}$, and the cathode layers LiF and Al were evaporated at a rate of 0.1 \AA/s and 10 \AA/s , respectively. The Electroluminescence (EL) characteristics of the devices were measured using a Spectrascan PR655 and a computer controlled Keithley 2400 light source meter. EQEs were calculated based on current density, brightness and EL Spectral.

Population ratio calculation of the conformations

For a molecule with more than one conformation, the population ratio of each conformation can be estimated by using Boltzmann distribution as the follow equation:¹

$$\%conformation_i = \frac{\text{Exp}\left(-\frac{E_i}{k_b T}\right)}{\sum_j \text{Exp}\left(-\frac{E_j}{k_b T}\right)} \quad \text{S1}$$

Where E is the conformational relative energy, T is the ambient temperature, and k_b is the Boltzmann constant.

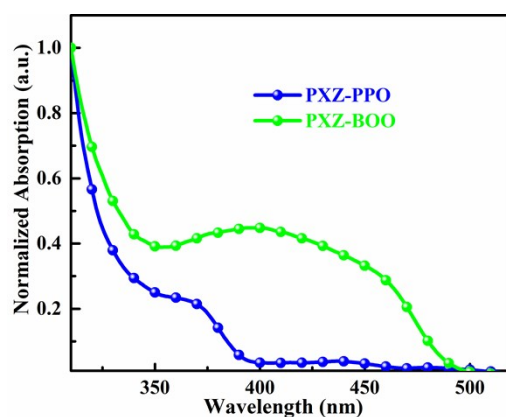


Fig. S1 Absorption spectra of the crystal samples of PXZ-PPO and PXZ-BOO.

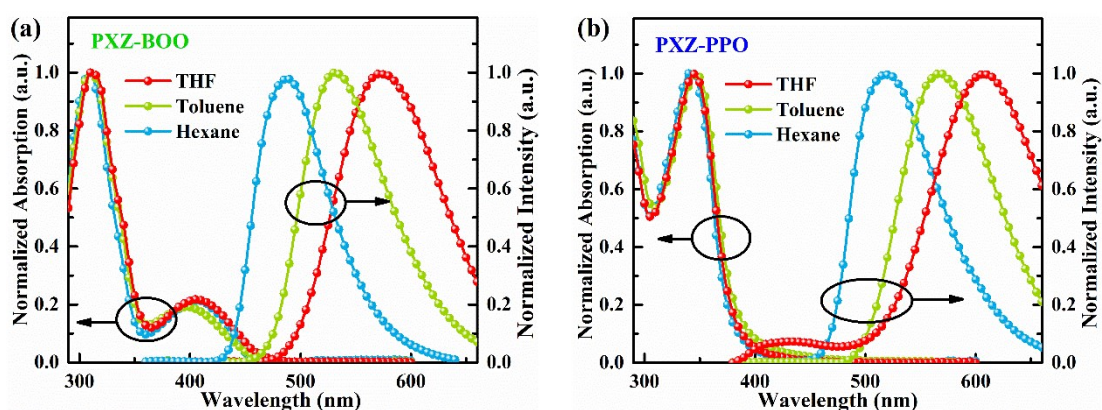


Fig. S2 Absorption and PL spectra of PXZ-BOO (a) and PXZ-PPO (b) at room temperature tetrahydrofuran (THF), toluene and hexane solvents. (Excited at 340 nm).

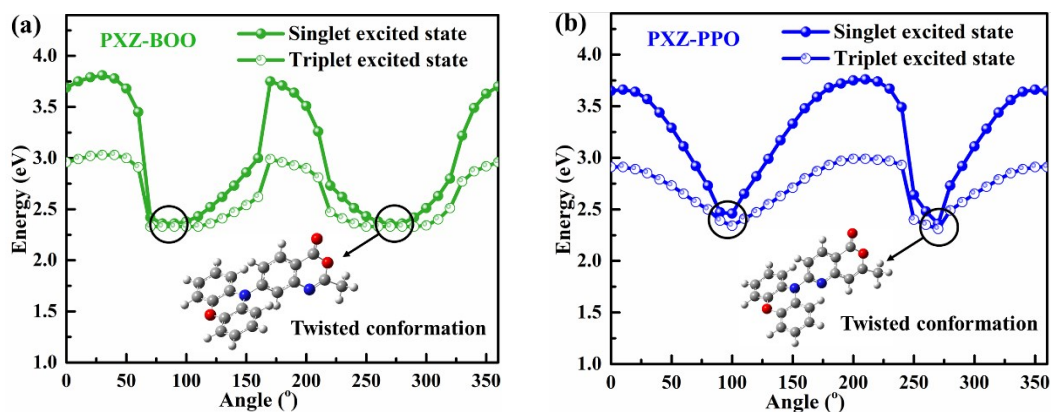


Fig. S3 The excited state energy levels of (a) PXZ-BOO; and (b) PXZ-PPO calculated via TD-DFT at the B3LYP/6-31G* level in THF; Black circles represent the twisted conformations.

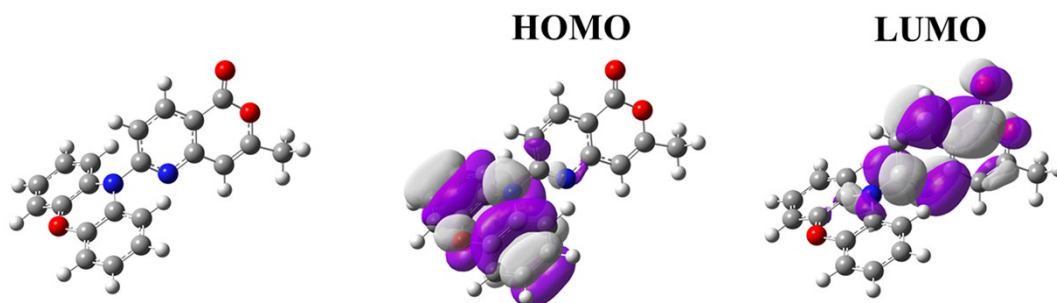


Fig. S4 Calculated spatial distributions of the HOMO/LUMO in the highly-twisted conformation of PXZ-PPO via DFT at the B3LYP/6-31G* level.

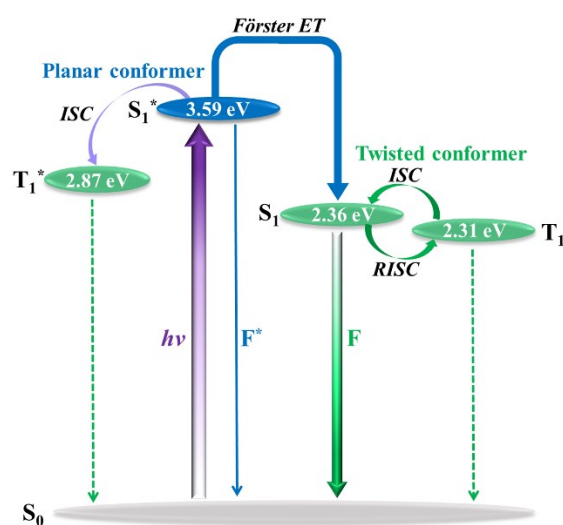


Fig. S5 The energy transfer process of PXZ-PPO after excitation; Excited state energy levels are calculated via TD-DFT at the B3LYP/6-31G* level in THF condition.

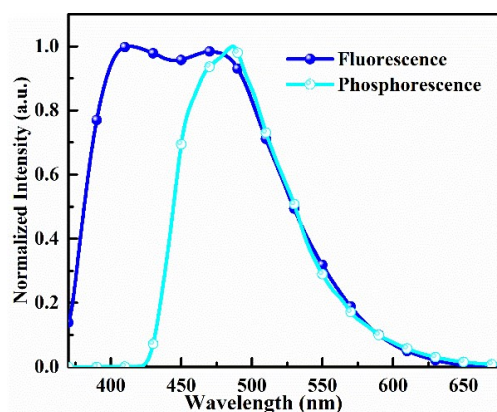


Fig. S6 Fluorescence and phosphorescence spectra of PXZ-PPO in THF at 77 K, excited at 340 nm.

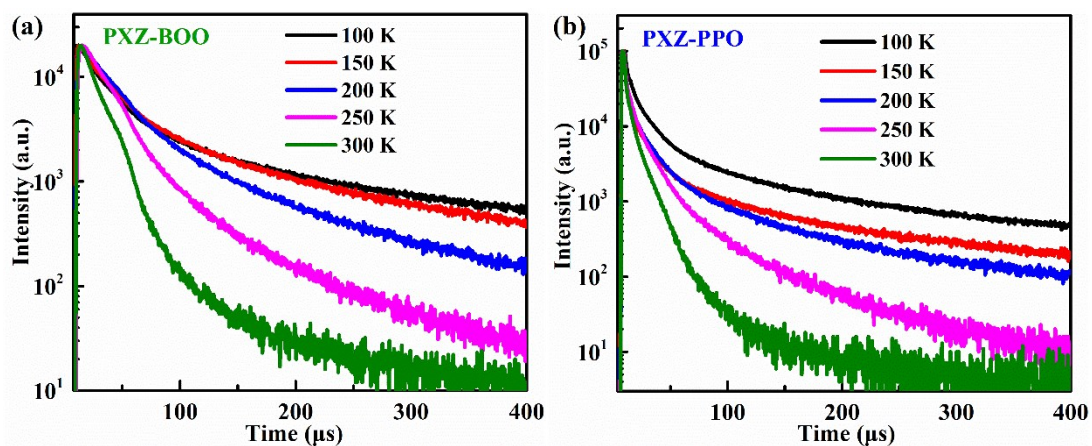


Fig. S7 Transient decay spectra of (a) PXZ-BOO and (b) PXZ-PPO 11.2% mixed in mCBP excited at 300 nm, measured at 520 nm.

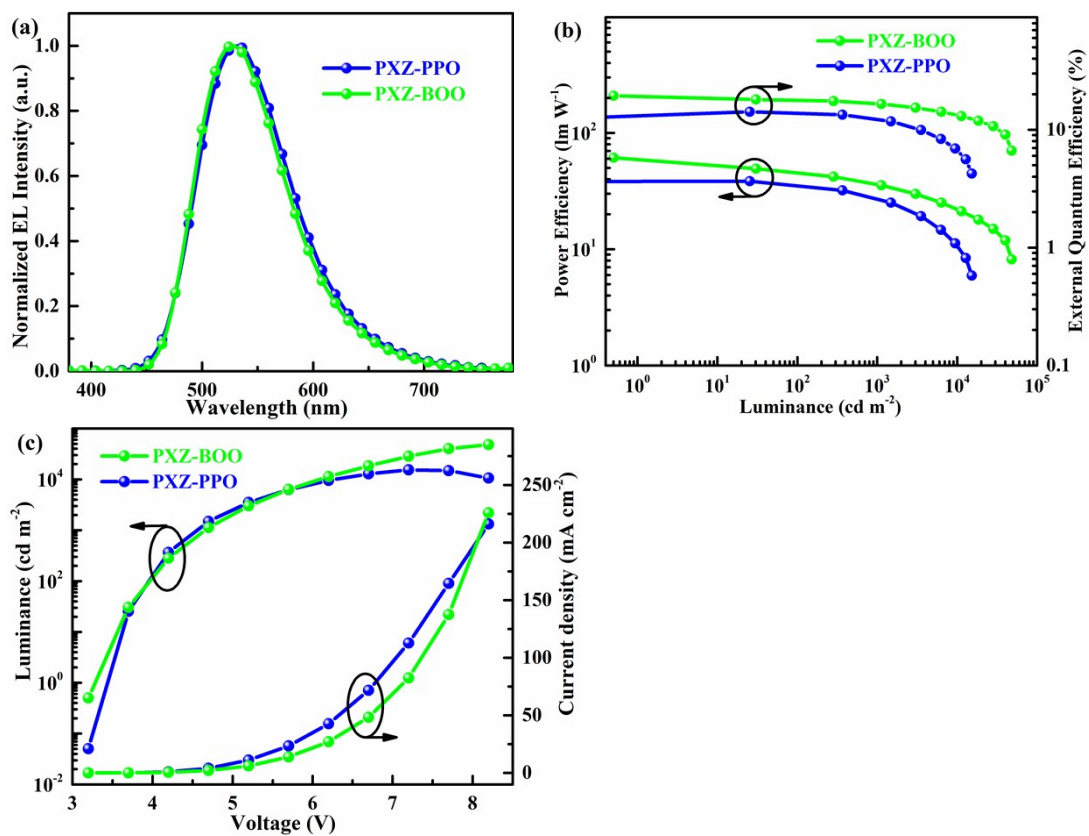


Fig. S8 EL performance of PXZ-PPO and PXZ-BOO based OLEDs, at concentration of 11.2 wt%.

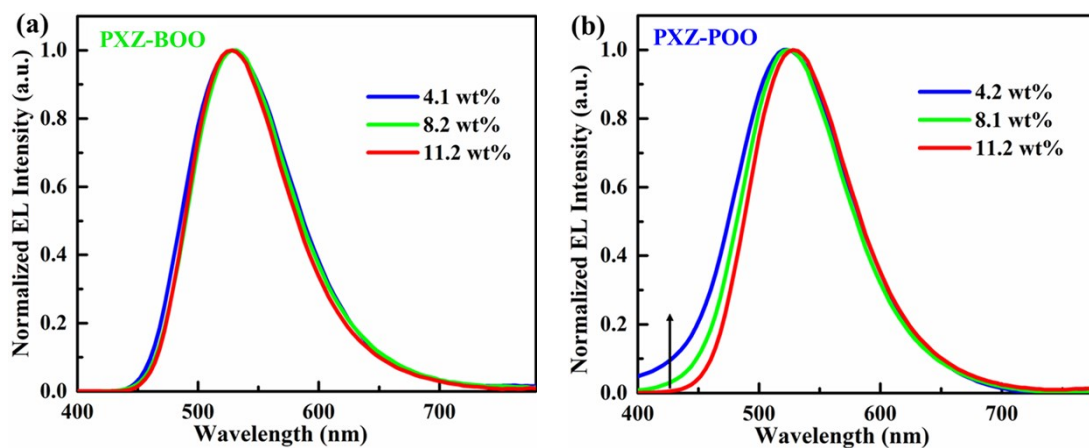


Fig. S9 EL intensity of (a) PXZ-BOO and (b) PXZ-PPO based OLEDs in different doping concentrations.

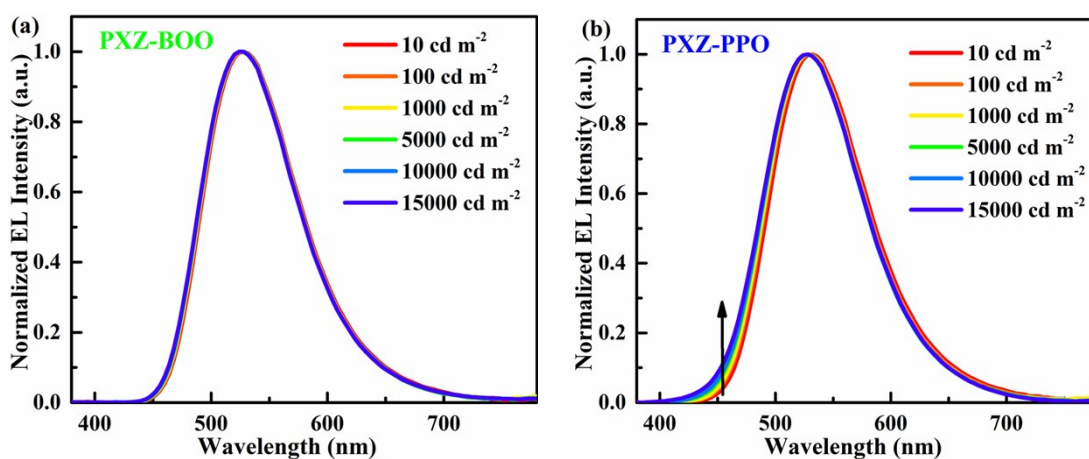


Fig. S10 EL intensity of (a) PXZ-BOO and (b) PXZ-PPO based OLEDs at different luminance, at concentration of 11.2 wt%.

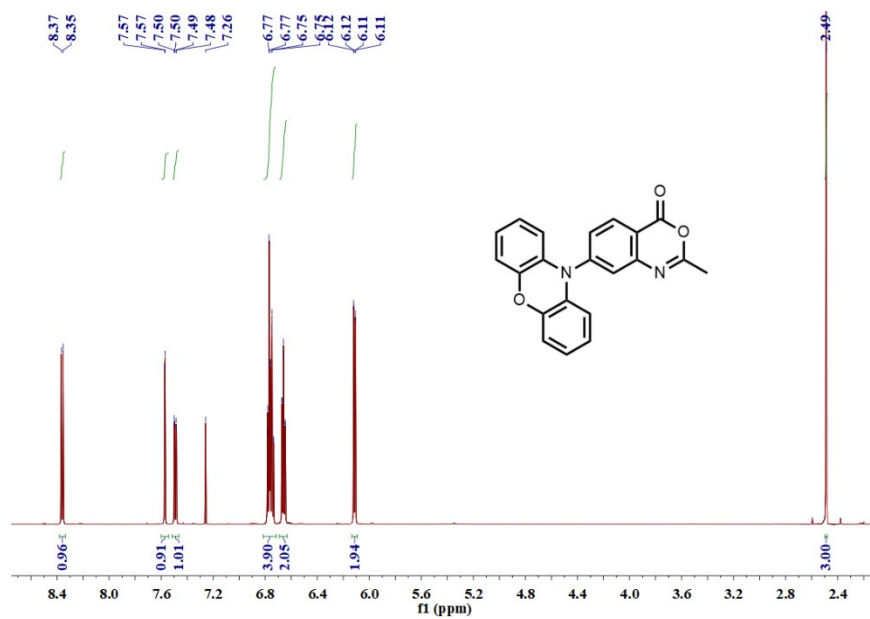


Fig. S11 ^1H NMR spectrum of PXZ-BOO in CDCl_3 .

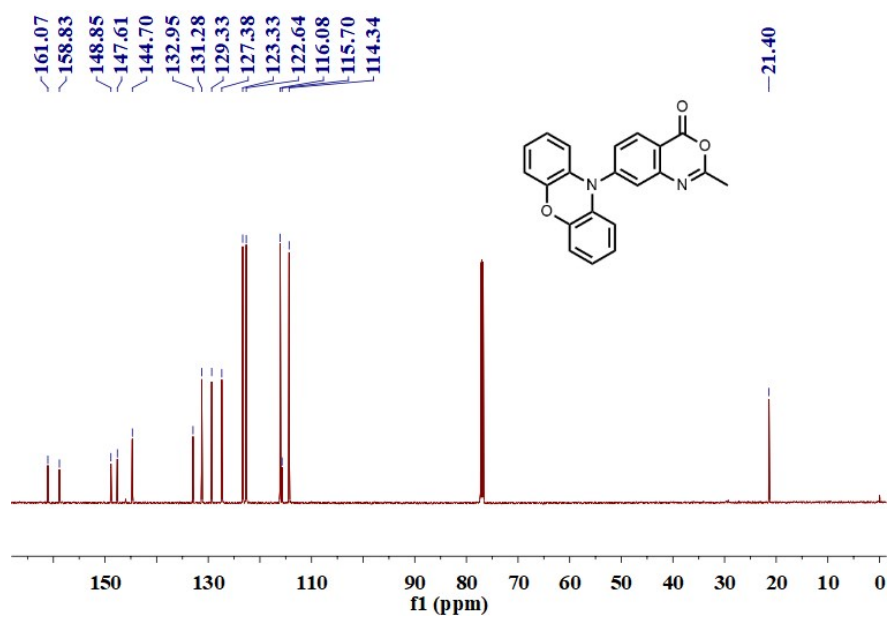


Fig. S12 ^{13}C NMR spectrum of PXZ-BOO in CDCl_3 .

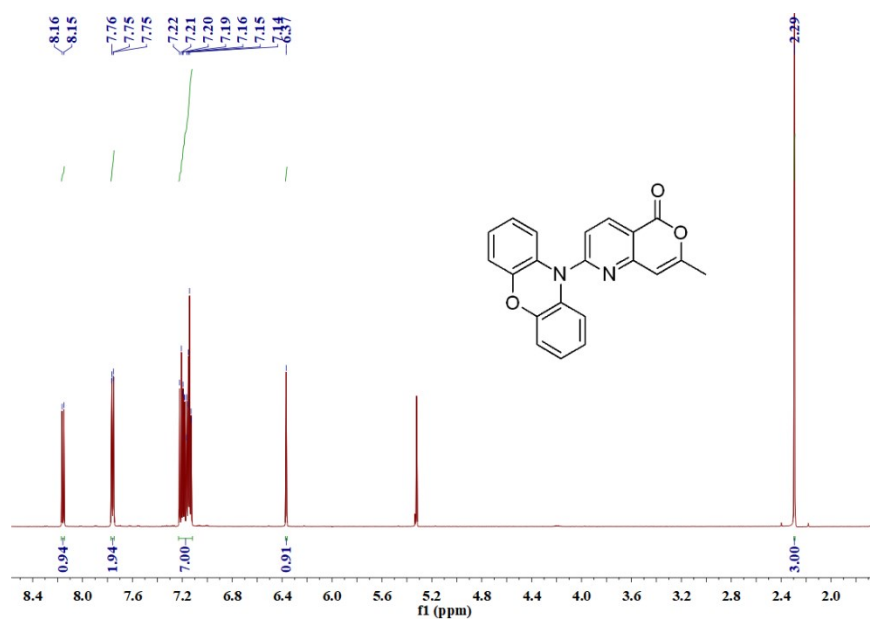


Fig. S13 ¹H NMR spectrum of PXZ-PPO in CD₂Cl₂.

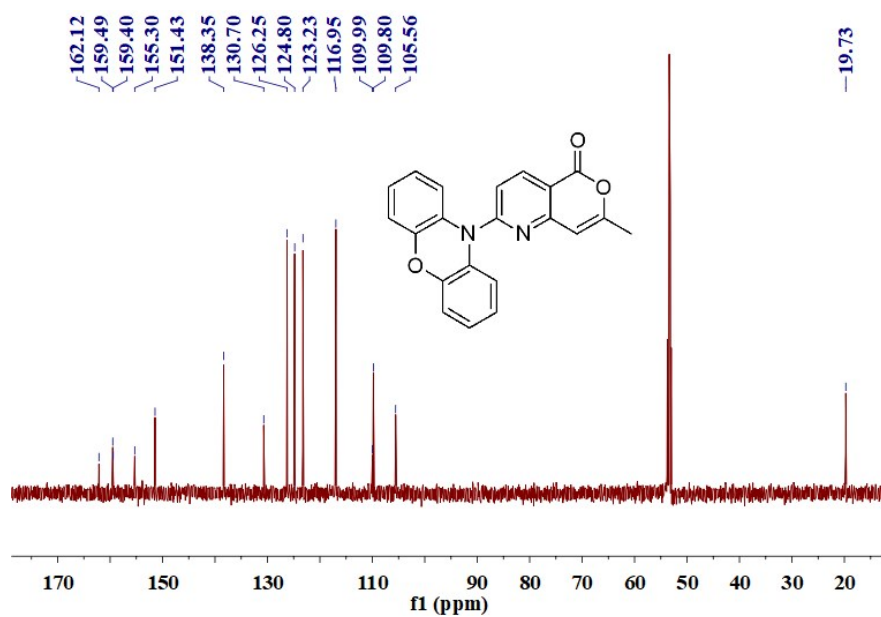


Fig. S14 ¹³C NMR spectrum of PXZ-PPO in CD₂Cl₂.

Table S1 Summary of the crystal data of PXZ-PPO and PXZ-BOO.

Parameter	PXZ-PPO	PXZ-BOO
CCDC	1942310	1942309

Empirical formula	$C_{10.5}H_7NO_{1.5}$	$C_{21}H_{14}N_2O_3$
Formula weight (g mol ⁻¹)	171.17	342.34
Temperature (K)	296(2)	193(2)
Crystal system	triclinic	triclinic
Space group	<i>P-1</i>	<i>P-1</i>
Unit cell dimensions	$a/\text{\AA} = 7.7616(7) \text{\AA}$ $b/\text{\AA} = 7.9306(7) \text{\AA}$ $c/\text{\AA} = 14.0253(13) \text{\AA}$ $\alpha/^\circ = 96.842(3)$ $\beta/^\circ = 100.695(4)$ $\gamma/^\circ = 110.912(3)$	$a/\text{\AA} = 4.2799(2) \text{\AA}$ $b/\text{\AA} = 11.3138(6) \text{\AA}$ $c/\text{\AA} = 17.3113(10) \text{\AA}$ $\alpha/^\circ = 102.246(2)$ $\beta/^\circ = 96.206(2)$ $\gamma/^\circ = 96.100(2)$
Volume (Å ³)	776.11(12)	807.14(7)
Z	2	2
ρ_{calc} g/cm ⁻³	0.732	1.409
μ (mm ⁻¹)	0.050	0.096
F(000)	178	356
Crystal size/mm ³	-	0.62 × 0.04 × 0.02
Radiation	MoK α ($\lambda = 0.71073$)	MoK α ($\lambda = 0.71073$)
2 θ range for data collection (°)	5.614 to 55.172	4.86 to 52.678
Index ranges	-10 ≤ h ≤ 10, -10 ≤ k ≤ 10, -18 ≤ l ≤ 18	-5 ≤ h ≤ 5, -14 ≤ k ≤ 14, -19 ≤ l ≤ 21
Reflections collected	35117	10324
Independent reflections	3576 [$R_{\text{int}} = 0.0623$, $R_{\text{sigma}} = 0.0335$]	3287 [$R_{\text{int}} = 0.0631$, $R_{\text{sigma}} = 0.0663$]
Data/restraints/parameters	3576/0/236	3287/0/236
Goodness-of-fit on F ²	1.058	1.044
Final R indices [$I \geq 2\sigma(I)$]	$R_1 = 0.0465$, wR ₂	$R_1 = 0.0514$, wR ₂

	=0.1356	=0.1231
R indices (all data)	R ₁ = 0.0701, wR ₂ = 0.1566	R ₁ = 0.0724, wR ₂ = 0.1389
Largest diff. peak and hole (e. Å ⁻³)	0.48/-0.49	0.20/-0.26

Table S2 The excited state energy levels of PXZ-PPO and PXZ-BOO in the nearly-planar and the highly-twisted conformations, calculated via TD-DFT at the B3LYP/6-31G* level in THF condition.

Compound	Conformation	S ₁ (eV)	T ₁ (eV)	ΔE _{ST} (eV)
PXZ-PPO	nearly-planar	3.59	2.87	0.72
	highly-twisted	2.36	2.31	0.05
PXZ-BOO	nearly-planar	3.75	2.99	0.76
	highly-twisted	2.36	2.33	0.03

Table S3 EL performances of OLEDs based on mCBP-doped 11.2 wt% PXZ-PPO and PXZ-BOO.

Device	V _{on} ^a (V)	L ^b (cd m ⁻²)	EQE _{max} ^c (%)	CE _{max} ^d (cd A ⁻¹)	PE _{max} ^e (lm W ⁻¹)	λ _{max} ^f (nm)	CIE ^f (x, y)
PXZ-PPO	3.4	15320	14.1	45.4	38.5	528	(0.32, 0.56)
PXZ-BOO	3.3	48220	19.4	62.3	61.2	528	(0.32, 0.56)

^a Turn-on voltage, calculated at luminance of 1 cd m⁻²; ^b Maximum luminance; ^c Maximum external quantum efficiency; ^d Maximum current efficiency; ^e Maximum power efficiency; ^f EL emission peak and Commission Internationale de L'Eclairage, measured at the luminance of 100 cd m⁻².

Reference

1 W. Li, X. Cai, B. Li, L. Gan, Y. He, K. Liu, D. Chen, Y.-C. Wu, S.-J. Su, *Angew. Chem. Int. Ed.*

2019, 58, 582-586.